Title

Damage Identification Study of a Seven-story Full-scale Building Slice Tested on the UCSD-NEES Shake Table

Journal

Structural Safety, 32(5)

ISSN

0167-4730

Authors

Moaveni, Babak
He, Xianfei
Resterpo, Jose I
et al.

Publication Date

2010-09-01

DOI

doi:10.1016/j.strusafe.2010.03.006

Peer reviewed

DAMAGE IDENTIFICATION STUDY OF A SEVEN-STORY FULL-SCALE BUILDING SLICE TESTED ON THE UCSD-NEES SHAKE TABLE

Babak Moaveni [a], **Xianfei He** [b], **Joel P. Conte** [c, 1], **Jose I. Restrepo** [c]

[a] *Department of Civil and Environmental Engineering, Tufts University, 200 College Avenue, Medford, MA 02155, United States*

[b] *AECOM Transportation, 999 Town & Country Road, Orange, CA 92868, United States*

[c] *Department of Structural Engineering, University of California, San Diego, 9500 Gilman Drive, La Jolla, CA 92093, United States*

ABSTRACT

A full-scale seven-story reinforced concrete building section was tested on the UCSD-NEES shake table during the period October 2005 - January 2006. The shake table tests were designed to damage the building progressively through four historical earthquake records. At various levels of damage, ambient vibration tests and low amplitude white noise base excitations with root-mean-square accelerations of 0.03g and 0.05g were applied to the building, which responded as a quasi-linear system with parameters evolving as a function of structural damage. Modal parameters (natural frequencies, damping ratios and mode shapes) of the building were identified at different damage levels based on the response of the building to ambient as well as low amplitude white noise base excitations, measured using DC coupled accelerometers. This paper focuses on damage identification of this building based on changes in identified modal parameters. A sensitivity-based finite element model updating strategy is used to detect, localize and quantify damage at each damage state considered. Three sets of damage identification results

1. Corresponding author. Tel.: +1 858-822-4545; fax: +1 858-822-2260. *E-mail address*: jpconte@ucsd.edu

are obtained using modal parameters identified based on ambient, 0.03g, and 0.05g RMS white noise test data, respectively. The damage identification results obtained in all three cases do not exactly coincide, but they are consistent with the concentration of structural damage observed at the bottom two stories of the building. The difference in the identified damage results is mainly due to the significant difference in the identified modal parameters used in the three cases. The assumption of a quasi-linear dynamic system is progressively violated with increasing level of excitation. Therefore, application of nonlinear FE model updating strategies is recommended in future studies to resolve the errors caused by structural response nonlinearity.

Keywords: Vibration-based damage identification; Experimental modal analysis; Modal parameters; Finite element model updating; Shake table tests.

INTRODUCTION

In recent years, structural health monitoring has received increasing attention in the civil engineering research community with the objective to develop methods able to identify structural damage at the earliest possible stage and to evaluate the remaining useful life of structures (damage prognosis). Vibration-based, non-destructive damage identification makes use of changes in dynamic characteristics (e.g., modal parameters) to identify structural damage. Experimental modal analysis (EMA) has been used as a technology for identifying modal parameters of a structure based on low amplitude vibration data. It should be emphasized that the success of damage identification based on EMA depends strongly on the accuracy and completeness of the identified structural dynamic properties. Extensive reviews on vibration-based damage identification were provided by Doebling et al. [1, 2] and Sohn et al. [3].

Damage identification consists of: (1) detecting the occurrence of damage, (2) localizing the damage areas, and (3) estimating the extent of damage in the various damage areas [4]. Numerous vibration-based methods to achieve these goals have been proposed in the literature. Salawu [5] presented a review on the use of changes in natural frequencies for the purpose of damage detection only. Pandey et al. [6] introduced the concept of using curvature mode shapes for damage localization. Methods based on changes in identified modal parameters to detect and localize damage have also been further developed for the purpose of damage quantification. Among these methods are strain-energy based methods [7] and the direct stiffness calculation method [8]. Another class of sophisticated methods consists of applying sensitivity-based finite element (FE) model updating for damage identification [9]. These methods update the physical parameters of a FE model of the structure by minimizing an objective function expressing the discrepancy between FE predicted and experimentally identified structural dynamic properties that are sensitive to damage such as natural frequencies and mode shapes. Optimum solutions of the problem are reached through sensitivity-based constrained optimization algorithms. In recent years, sensitivity-based FE model updating methods have been applied successfully for condition assessment of structures [10, 11].

A full-scale seven-story reinforced concrete building section was tested on the UCSD-NEES shake table in the period October 2005 - January 2006. The objective of this test program was to verify the seismic performance of a mid-rise reinforced concrete wall building designed for lateral forces obtained from a displacement-based design method, which are significantly smaller than those dictated by current force-based seismic design provisions in the United States [12, 13]. The shake table tests were designed to damage the building progressively through several historical seismic motions. At various levels of damage, ambient vibration tests were per-

formed and several low amplitude white noise base excitations were applied through the shake table to the building which responded as a quasi-linear system with dynamic parameters evolving as a function of structural damage. Different input-output and output-only system identification methods were used to estimate modal parameters (natural frequencies, damping ratios and mode shapes) of the building in its undamaged (baseline) and various damaged states for three different levels of input excitation (i.e., ambient, 0.03g and 0.05g root-mean-square white noise base excitations) [14].

In this study, a FE model updating strategy is applied for damage identification of the building in various damaged states. The objective function for damage identification is defined as a combination of natural frequency and mode shape residuals measuring the discrepancy between the FE predicted and experimentally identified modal parameters. Three cases of damage identifications are considered in this study, namely (1) residuals are constructed from the modal parameters identified based on ambient vibration data, (2) residuals are formed using the modal parameters identified based on 0.03g root-mean-square (RMS) white noise base excitation test data, and (3) residuals are formed using the modal parameters identified based on 0.05g RMS white noise base excitation test data. The damage identification results obtained from these three cases are compared to each other and also to the damage observed in the building (from pictures, video cameras, and inferred from strain sensors).

TEST SPECIMEN, TEST SETUP AND DYNAMIC EXPERIMENTS

Seven-Story Reinforced Concrete Building Slice

The test structure which represented a section of a full-scale reinforced concrete wall building consisted of a main wall (web wall), a back wall perpendicular to the main wall (flange

wall) for transversal stability, a concrete slab at each floor level (except at the base), an auxiliary post-tensioned column to provide torsional stability, and four gravity columns to transfer the weight of the slabs to the shake table platen. Slotted slab connections were placed between the web and flange walls at floor levels to minimize the moment transfer between the two walls, while allowing the transfer of the in-plane diaphragm forces. Figures 1 shows the building mounted on the shake table. More details about the building can be found in [12, 13].

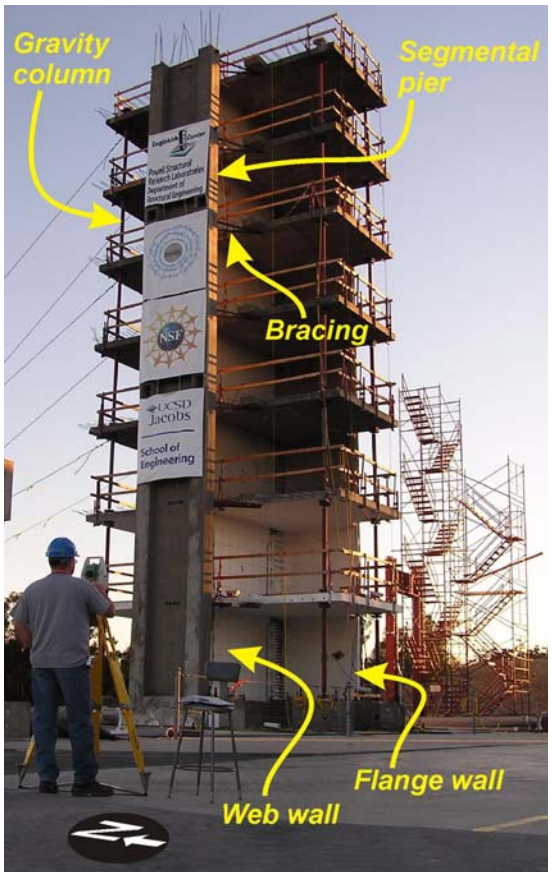

Fig. 1 Test structure

Instrumentation Layout

The building was instrumented with a dense array of more than 430 data channels from DC coupled accelerometers, strain gages, potentiometers, and linear variable displacement transducers (LVDTs) sampled simultaneously using a nine-node distributed data acquisition system.

The technical characteristics of the accelerometers are: MEMS-Piezoresistive MSI model 3140, amplitude range: +/-5g, frequency range (min): 0-300Hz, voltage sensitivity: 400mV/g. The data acquisition system used consisted of nine 16-bit resolution National Instruments PXI chassis. Each chassis had eight SCXI 1520 modules which were individually configured to handle eight channels of strain gages, accelerometers, relative displacement, and/or pressure sensors.

In this study, data from 14 longitudinal acceleration channels (on the web wall at each floor level and at mid-height of each story) were used to identify the damage at different states of the building. The measured acceleration responses were sampled at a rate of 240Hz resulting in a Nyquist frequency of 120Hz, which is much higher than the modal frequencies of interest in this study (< 25Hz). These measured data were band-pass filtered between 0.5Hz and 25Hz using a high order (1024) FIR filter. Figure 2 shows the Fourier Amplitude Spectra (FAS) of two filtered acceleration time histories recorded at floor levels 1 (first floor above the table) and 7 (roof) during a 0.03*g* RMS white noise base excitation test (left column) and an ambient vibration test (right column) performed on the building in its undamaged state. From this figure, it is observed that: (1) the FAS plots are very jagged/noisy which may be due to rattling of many loose connections especially from the slackness between the threaded rod and the nut in the gravity columns (1.5 mm of slackness) when they go from tension to compression or vice versa as well as the slackness at both ends of the steel braces connecting the slabs to the post-tensioned column; (2) the first longitudinal vibration mode has a predominant contribution to the measured response, especially at the higher floors, which renders the identification of higher (than the first longitudinal) modes more difficult; and (3) the FAS of the acceleration response histories at the first floor appear to have a drop in amplitude at around 11.5 Hz which is due to the application of a notch filter in the

control loop of the table to reduce the effects of the oil column resonance. Mechanical characteristics of the shake table are available in [15].

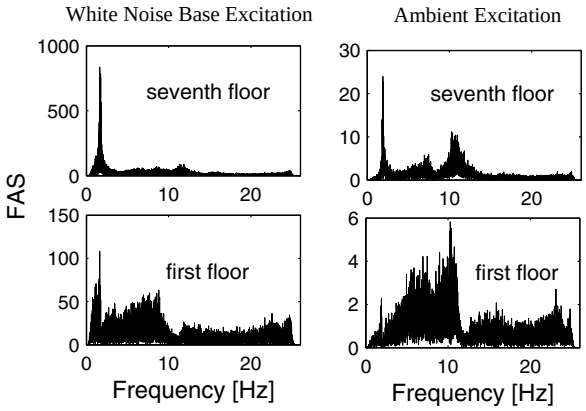

Fig. 2 Fourier Amplitude Spectra of acceleration response measurements at the first and seventh (roof) floors due to 0.03*g* RMS white noise base excitation (left) and ambient excitation (right)

Dynamic Tests Performed

A sequence of dynamic tests (68 tests in total) was applied to the building during the test period including ambient vibration tests, free vibration tests, and forced vibration tests (white noise and seismic base excitations) using the UCSD-NEES shake table. The building was damaged progressively through four historical ground motion records and the modal parameters of the building were identified at various damage states using different state-of-the-art system identification methods and different dynamic test data.

The four historical earthquake records applied to the building were: (1) longitudinal component of the 1971 San Fernando earthquake (M_w = 6.6) recorded at the Van Nuys station (EQ1), (2) transversal component of the 1971 San Fernando earthquake recorded at the Van Nuys station (EQ2), (3) longitudinal component of the 1994 Northridge earthquake (M_w = 6.7) recorded at the Oxnard Boulevard station in Woodland Hill (EQ3), and (4) 360 degree component of the 1994

Northridge earthquake recorded at the Sylmar station (EQ4). The input white noise base excitation consisted of two 8 minute long realizations of a banded white noise (0.25-25Hz) process with root-mean-square (RMS) amplitudes of 0.03g and 0.05g, respectively. Table 1 reports the dynamic tests used in the present study on vibration-based damage identification of the building at various damage states.

Table 1 Dynamic tests used in this study
(WN: white noise base excitation test and AV: ambient vibration test)

Test No.	Date	Test Description	State
39	11/21/05	8min WN (0.03*g*) + 3min AV	S0
40	"	EQ1	
41	"	8min WN (0.03*g*) + 3min AV	S1
42	"	8min WN (0.05*g*)	S1
43	"	EQ2	
46	11/21/05	8min WN (0.03*g*) + 3min AV	S2
47	"	8min WN (0.05*g*)	S2
48	"	EQ3	
49	"	8min WN (0.03*g*) + 3min AV	S3.1
50	"	8min WN (0.05*g*)	S3.1
61	1/14/06	8min WN (0.03*g*) + 3min AV	S3.2
62	"	EQ4	
64	1/18/06	8min WN (0.03*g*) + 3min AV	S4
65	"	8min WN (0.05*g*)	S4

SYSTEM IDENTIFICATION RESULTS

Modal parameters of the building were identified based on measured data from low amplitude dynamic tests (i.e., ambient vibration tests and white noise base excitation tests) at various

damage states of the building [14]. State S0 is defined as the undamaged (baseline) state of building before its exposure to the first seismic excitation (EQ1), while states S1, S2, S3 and S4 correspond to the state of building after exposure to the first (EQ1), the second (EQ2), the third (EQ3), and the fourth (EQ4) seismic excitation, respectively (see Table 1). State S0 does not correspond to the uncracked state of the building, since the latter had already been subjected to low-amplitude white noise base excitations (0.02-0.03g RMS) for the purposes of checking the instrumentation and data acquisition system and tuning the shaking table controller. It should be noted that during state S3, the bracing system between the slabs of the building and the post-tensioned column was stiffened. Therefore, state S3 is subdivided into S3.1 (before modification of the braces) and S3.2 (after modification of the braces). In this study, the natural frequencies and mode shapes of the first three longitudinal vibration modes are used for damage identification of the building at states S1, S2, S3.1, and S4. Figure 3 shows the real part of the complex-valued mode shapes of the first three longitudinal vibration modes (1st-L, 2nd-L, 3rd-L) of the building identified based on ambient vibration data from Test 39 at state S0.

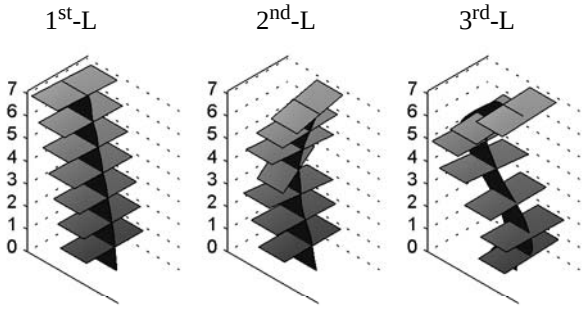

Fig. 3 Longitudinal mode shapes of the building at state S0 obtained based on ambient vibration data

Table 2 reports the natural frequencies of the three longitudinal vibration modes (1^{st}-L, 2^{nd}-L, 3^{rd}-L) identified based on acceleration data from ambient vibration, 0.03g, and 0.05g RMS

white noise base excitation tests, respectively, at all the damage states considered. Vibration mode shape normalization was performed by projecting all mode shape components onto their major principal axis (in the complex plane) and then scaling this projected mode shape vector for a unit value of its largest component. This normalization results in real valued mode shapes which are more suitable to be used in FE model updating. From Table 2, it is observed that the identified natural frequencies decrease with increasing level of damage. Note that the identified modal damping ratios do not exhibit a clear trend with increasing structural damage.

Table 2 Natural frequencies [Hz] identified based on acceleration data from ambient vibration, 0.03g, and 0.05g RMS white noise base excitation tests

State	Ambient Vibration			0.03g RMS White Noise			0.05g RMS White Noise		
	1^{st}-L mode	2^{nd}-L mode	3^{rd}-L mode	1^{st}-L mode	2^{nd}-L mode	3^{rd}-L mode	1^{st}-L mode	2^{nd}-L mode	3^{rd}-L mode
S0	1.91	10.51	24.51	1.71	11.05	24.31	NA	NA	NA
S1	1.88	10.21	24.31	1.54	10.98	24.28	1.40	11.38	24.29
S2	1.67	10.16	22.60	1.24	11.11	21.59	1.14	10.24	22.46
S3.1	1.44	9.23	21.82	1.14	9.77	19.68	1.06	10.23	18.98
S4	1.02	5.67	15.09	0.88	4.81	13.29	0.81	4.62	13.29

FINITE ELEMENT MODEL UPDATING FOR DAMAGE IDENTIFICATION

In this study, a sensitivity-based FE model updating strategy [16] is used to identify (detect, localize and quantify) the damage in the building at the different states considered. The residuals used in the updating procedure are based on the identified natural frequencies and mode shapes for the first three longitudinal modes of the building. Damage in the building is identified as a change in material stiffness (effective modulus of elasticity) of the finite elements in the different substructures of the FE model used for damage identification. For the purpose of damage

identification, the effective moduli of elasticity of elements in various substructures (each assumed to have a uniform value of the effective modulus of elasticity) are updated at each considered state of the building. In each case, the effective moduli of elasticity of the various substructures are updated from the reference/baseline model to the state considered through constrained minimization of an objective function.

Objective Function

The objective function for damage identification is defined as

$$\begin{aligned} \min_{\boldsymbol{\theta}} f(\boldsymbol{\theta}) &= \mathbf{r}(\boldsymbol{\theta})^{\mathrm{T}}\mathbf{W}\mathbf{r}(\boldsymbol{\theta}) + (\mathbf{a}(\boldsymbol{\theta}) - \mathbf{a}^{0})^{\mathrm{T}}\mathbf{W}^{\mathrm{a}}(\mathbf{a}(\boldsymbol{\theta}) - \mathbf{a}^{0}) \\ &= \sum_{i}[w_i r_i(\boldsymbol{\theta})^2] + \sum_{k}[w_k^{\mathrm{a}}(a_k(\boldsymbol{\theta}) - a_k^{0})^2] \end{aligned} \tag{1}$$

where $\boldsymbol{\theta}$ = set of physical parameters (i.e., effective moduli of elasticity) which must be adjusted in order to minimize the objective function; $\mathbf{r}(\boldsymbol{\theta})$ = residual vector containing the differences between analytically computed (FE predicted) and experimentally identified modal parameters; $\mathbf{a}(\boldsymbol{\theta})$ = vector of dimensionless damage factors representing the level of damage in each of the substructures of the FE model used for damage identification (see next section); $\mathbf{a}^0$ = vector of initial damage factors used as starting point in the optimization process. At each considered state of the building, $\mathbf{a}^0$ is selected as the identified damage factors for the previous state and $\mathbf{a}^0 = \mathbf{0}$ for state S1. In Eq. (1), $\mathbf{W}$ is a weighting matrix for modal residuals, a diagonal weighting matrix with each diagonal coefficient assigned based on the estimation uncertainty (coefficient-of-variation) of the natural frequency of the corresponding mode [17] as well as the modal contribution of this mode. Weight factors assigned to mode shape residuals are equal to the weight factor of that

mode natural frequency, normalized/divided by the number of mode shape residuals for each mode. Table 3 presents the assigned weight factors for different vibration modes at each damage state and for different cases of damage identification. Identical weights are used for the second and third cases of damage identification.

Table 3 Weight factors assigned to natural frequency residuals of different vibration modes at different damage states

State	Ambient Vibration / White Noise		
	1^{st}-L mode	2^{nd}-L mode	3^{rd}-L mode
S0	1.0/1.0	0.2/0.2	0.8/0.5
S1	1.0/1.0	0.1/0.2	0.5/0.8
S2	1.0/1.0	0.25/0.2	0.375/0.4
S3.1	1.0/1.0	0.2/0.3	0.8/0.8
S4	1.0/1.0	0.5/0.4	0.75/0.4

The first vibration mode contributes predominantly to the dynamic response of the building at all states considered, and therefore its corresponding residuals are assigned the largest weights among the three vibration modes. Still in Eq. (1), $\mathbf{W}^{a}$ is a weighting matrix for damage factors, a diagonal weighting matrix with each diagonal coefficient defining the relative cost (or penalty) of changing/updating the corresponding damage factor. The weights for damage factors reduce the estimation error of the damage factors in the presence of estimation uncertainty in the modal parameters, especially for the substructures with updating parameters to which the employed residuals are less sensitive. In this study, these weight are set to $w_k^a = 0.01 \times w_1$ with $k = 1, \ldots, n_{sub}$ where n_{sub} denotes the number of substructures considered in the FE model

updating process and w_1 is the weight assigned to the modal residual corresponding to the natural frequency of the first mode. A combination of residuals in natural frequencies and mode shape components is used in the objective function as

$$\mathbf{r}(\boldsymbol{\theta}) = \begin{bmatrix} \mathbf{r}_f(\boldsymbol{\theta}) \\ \mathbf{r}_s(\boldsymbol{\theta}) \end{bmatrix} \tag{2}$$

in which $\mathbf{r}_f(\boldsymbol{\theta})$ and $\mathbf{r}_s(\boldsymbol{\theta})$ represent the eigen-frequency and mode shape residuals, respectively, as

$$\mathbf{r}_f(\boldsymbol{\theta}) = \left[\frac{\lambda_j(\boldsymbol{\theta}) - \tilde{\lambda}_j}{\tilde{\lambda}_j} \right], \qquad \mathbf{r}_s = \left[\frac{\phi_j^l(\boldsymbol{\theta})}{\phi_j^r(\boldsymbol{\theta})} - \frac{\tilde{\phi}_j^l}{\tilde{\phi}_j^r} \right], \qquad l \neq r, \qquad j = 1, \ldots, n_m \tag{3}$$

where $\lambda_j(\boldsymbol{\theta})$ and $\tilde{\lambda}_j$ denote the analytical (FE predicted) and experimentally identified eigenvalues, respectively, corresponding to the j^{th} vibration mode with $\lambda_j(\boldsymbol{\theta}) = \omega_j^2$ and ω_j = natural circular frequency; $\boldsymbol{\phi}_j(\boldsymbol{\theta})$ and $\tilde{\boldsymbol{\phi}}_j$ denote the analytical (FE predicted) and experimentally identified mode shape vectors, respectively. It should be noted that for each vibration mode, the mode shapes $\boldsymbol{\phi}_j(\boldsymbol{\theta})$ and $\tilde{\boldsymbol{\phi}}_j$ are normalized in the same way, i.e., scaled to a reference component. In Eq. (3), the superscript *r* indicates the reference component of a mode shape vector (with respect to which the other components of the mode shape are normalized), the superscript *l* refers to the mode shape components that are used in the FE model updating process (i.e., at the locations and in the directions of the sensors), and n_m denotes the number of vibration modes considered in the damage identification process. In this study, the natural frequencies and mode shapes of the first three longitudinal vibration modes of the building (see Figure 3) are used to form the residual vec-

tor $\mathbf{r}(\boldsymbol{\theta})$ which has a total of 42 residual components (based on 14 channels of acceleration response measurements) consisting of 3 eigen-frequency and $3 \times (14 - 1) = 39$ mode shape component residuals, respectively.

Damage Factors and Modal Residual Sensitivities

In the process of FE model updating, the material stiffness (i.e., effective modulus of elasticity) of each of the damage substructures are used as an updating parameter in the FE model of the building. Instead of using directly the absolute value of each updating parameter, a dimensionless damage factor is defined as

$$\mathbf{a}(k) = \frac{\mathrm{E}^{k}_{\text{undamaged}} - \mathrm{E}^{k}_{\text{damaged}}}{\mathrm{E}^{k}_{\text{undamaged}}} \tag{4}$$

where E^{k} is the effective modulus of elasticity of all finite elements in substructure k ($k = 1, \ldots, \mathrm{n}_{\text{sub}}$). Thus, the damage factor $\mathbf{a}(k)$ indicates directly the level of damage (i.e., relative change in effective modulus of elasticity) in substructure k when FE model updating is used for structural damage identification. The sensitivity of the modal residuals with respect to the damage factor $\mathbf{a}(k)$ can be obtained from Eq. (3) using the modal parameter sensitivities as

$$\frac{\partial \mathbf{r}_{\mathrm{f}}}{\partial \mathbf{a}(k)} = \left[\frac{1}{\tilde{\lambda}_j} \frac{\partial \lambda_j}{\partial \mathbf{a}(k)} \right] \quad \text{and} \quad \frac{\partial \mathbf{r}_{\mathrm{s}}}{\partial \mathbf{a}(k)} = \left[\frac{1}{\phi_j^r} \frac{\partial \phi_j^l}{\partial \mathbf{a}(k)} - \frac{\phi_j^l}{(\phi_j^r)^2} \frac{\partial \phi_j^r}{\partial \mathbf{a}(k)} \right] \qquad (l \neq r) \tag{5}$$

where the modal sensitivities $\frac{\partial \lambda_j}{\partial \mathbf{a}(k)}$ and $\frac{\partial \boldsymbol{\phi}_j}{\partial \mathbf{a}(k)}$ are available in [18]. Notice that according to Eq. (5), the sensitivity of the reference mode shape component with respect to $\mathbf{a}(k)$ equals zero as it should be.

Optimization Algorithm

The optimization algorithm used to minimize the objective function defined in Eq. (1) is a standard Trust Region Newton method [19], which is a sensitivity-based iterative method available in the MATLAB optimization Toolbox [20]. In this study, the damage factors were constrained to remain in the selected range [0% - 95%] at all states considered. The optimization process was performed using the "fmincon" function in Matlab, with the Jacobian matrix and a first-order estimate of the Hessian matrix calculated based on the analytical sensitivities of the modal residuals to the updating variables as given in Eq. (5). The use of the analytical Jacobian, rather than the Jacobian estimated through finite difference calculations, increases significantly the efficiency of the computational minimization of the objective function.

Finite Element Modeling of Test Structure in FEDEASLab

A three dimensional linear elastic FE model of the building was developed using a general-purpose FE structural analysis program, FEDEASLab [21] as shown in Figure 4(a). This FE model includes 340 nodes and 322 linear elastic shell and truss elements. A four-node linear elastic flat shell element (with four Gauss integration points) borrowed from the FE literature [22, 23] was implemented in FEDEASLab in order to model the web wall, flange wall, concrete slabs, and the post-tensioned column [24]. In this FE model, the web wall is modeled using 16 shell elements at each of the bottom three stories, 8 shell elements at the 4^{th} story, and 4 shell elements at each of the top three stories. The floor slabs are modeled using 24 (4×6 grid) shell elements for each of the first three floors and 12 (2×6 grid) shell elements for each of the higher floors (4 to 7). The flange wall and the post-tensioned column are modeled using 8 (2×4 grid) and 10 (2×5

grid) shell elements per story, respectively. The gravity columns and braces connecting the post-tensioned column to the building slabs are modeled using truss elements. The inertia properties of the building are discretized into lumped translational masses at each node of the FE model. This initial FE model of the building section is based on the measured structural material properties (i.e., average material properties over 2 samples per story) and blue prints of the building. Table 4 reports the average measured moduli of elasticity (through concrete cylinder tests) at various heights (stories) of the building, which are used in its initial FE model.

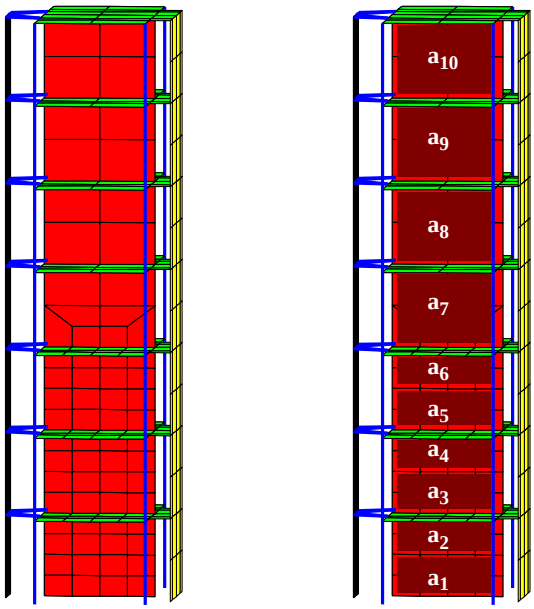

(a) (b)

Fig. 4 (a) FE model of test structure in FEDEASLab, and (b) definition of substructures along the web wall used for damage identification

Table 4 Measured and effective moduli of elasticity of structural components at different substructures of initial and reference FE models

Substructure	Effective Moduli of Elasticity [GPa]		
	Initial FE model	Reference FE model based on ambient vibration data	Reference FE model based on white noise test data
Web wall, 1st story (bot.)	24.5	17.1	22.0
Web wall, 1st story (top)	24.5	21.6	17.5
Web wall, 2nd story (bot.)	26.0	27.4	21.1
Web wall, 2nd story (top)	26.0	25.9	20.8
Web wall, 3rd story (bot.)	34.8	35.3	35.1
Web wall, 3rd story (top)	34.8	37.5	41.8
Web wall, 4th story	30.2	33.9	42.4
Web wall, 5th story	28.9	28.4	36.9
Web wall, 6th story	32.1	34.4	18.2
Web wall, 7th story	33.5	34.6	40.7
Slab, 1st floor	24.5	22.9	23.3
Slab, 2nd floor	26.0	24.6	23.6
Slab, 3rd floor	34.8	35.6	28.7
Slab, 4th floor	30.2	26.2	34.1
Slab, 5th floor	28.9	25.5	30.3
Slab, 6th floor	32.1	28.0	27.9
Slab, 7th floor	33.5	28.9	23.9
Base spring	1.56 GN-m/rad	fixed	1.81 GN-m/rad

DAMAGE IDENTIFICATION

In this study, three cases of damage identification are performed using the FE model updating algorithm described above. These three cases are based on three different sets of identified modal parameters of the building, namely (1) the modal parameters identified based on ambi-

ent vibration data, (2) the modal parameters identified based on 0.03g RMS white noise base excitation test data, and (3) the modal parameters identified based on 0.05g RMS white noise base excitation test data. In each of these cases, the first step to identify damage in the building consists of obtaining a reference/baseline FE model based on the modal parameters identified at the undamaged (or baseline) state of the building (S0). In this step, the initial FE model is updated to match the identified modal parameters at the undamaged state of the building by updating the stiffness (effective moduli of elasticity) of seventeen (in the first case of damage identification) or eighteen (in the second and third cases) substructures. The effective modulus of elasticity is assumed to be uniform/constant over each substructure. Therefore all finite elements of a substructure share the same value of the effective modulus of elasticity of concrete. It should be noted that the second and third cases of damage identification use the same reference FE model. This is due to the fact that the higher amplitude (0.05g RMS) white noise base excitation was not applied to the building at its undamaged state S0.

The seventeen substructures used in the calibration of the initial FE model to the reference FE model during the first damage identification case are defined by ten substructures along the web wall (six along the first three stories, every half story each, and four along the higher stories, every story each) as shown in Figure 4(b), and seven substructures consisting each of a floor slab. The eighteen substructures used in the second and third damage identification cases consist of the same seventeen substructures as those employed in the first damage identification case and a rotational spring at the base of the web wall. This rotational spring accounts for (1) the flexibility of the shake table platen, hydraulic bearings, foundation block (of shake table), and surrounding soil system, and (2) the localized rotation manifested at the base of the web wall (interface between web wall and pedestal) and caused by bar bond slip of the wall longitudinal reinforcing bars

anchored in the wall pedestal. It should be noted that the rotation at the base of the web wall played a non-negligible role in the response of the building during the white noise base excitation tests and the earthquake tests [13], while it was insignificant during the ambient vibration tests.

The effective moduli of elasticity of the various substructures obtained based on the modal parameters identified at the undamaged state S0, referred to herein as reference values, are reported in Table 4 for both cases of ambient vibration and 0.03g white noise test data together with the corresponding measured values of the concrete modulus of elasticity (obtained from 0.15 m diameter by 0.30 m tall cylinders tested under uniaxial compression on the day of the test) used in the initial FE model. During calibration of the initial FE model to the reference FE model (for both cases of using ambient vibration and 0.03g RMS white noise test data) the "damage factors" were constrained in the range $[-\infty, 1]$ in order to result in positive effective moduli of elasticity. From the results reported in Table 4, it is observed that for each substructure, the reference (calibrated) effective moduli of elasticity (for both reference models) differ from the corresponding measured (initial) values. This is due to the fact that the updating parameters (moduli of elasticity) act as effective moduli of elasticity reflecting the overall stiffness of the building, including the contributions of other structural components such as flange wall, post-tensioned column and gravity columns for which the stiffness parameters are not calibrated/updated. From Table 4, it is also seen that the reference values obtained for the two reference FE models (based on ambient vibration and 0.03g RMS white noise test data, respectively) are different. This is due to the fact that the building under 0.03g RMS white noise base excitation behaves as a cracked reinforced concrete building in contrast to the mainly uncracked behavior of the building under ambient excitation.

Case I: Damage Identification Based on Ambient Vibration Test Data

In this case of damage identification, once the reference model is obtained, 10 updating parameters (corresponding to 10 substructures) are updated from the reference FE model (at the undamaged/baseline state S0) to states S1, S2, S3.1, and S4. These 10 substructures represent the web wall, 6 along the first three stories (two per story) and 4 along the higher stories (one per story) as shown in Figure 4(b). The values of the stiffness parameters of the remaining substructures are kept fixed at the corresponding values in the reference FE model. For each of the considered states of the building, the natural frequencies and mode shapes of the first three longitudinal vibration modes are used in the objective function for damage identification, resulting in a residual vector with 42 components (i.e., 3 natural frequencies and 3 vibration mode shapes with $14 - 1 = 13$ components each).

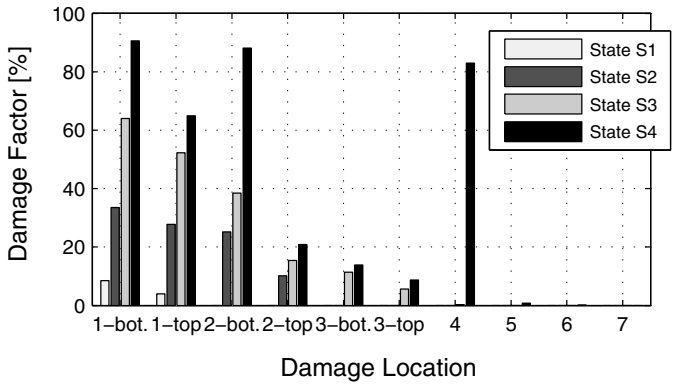

Fig. 5 Identified damage factors at various substructures for damage identification Case I (based on ambient vibration data)

In updating the FE model at each considered damage state of the building, the k^{th} dimensionless damage factor was constrained to be in the range $[\mathbf{a}_0^{Si}(k), 0.95]$, with $\mathbf{a}_0^{Si}(k)$ denoting the initial value of the damage factor of the k^{th} substructure at states Si = S1, S2, S3.1, S4. At each

state considered, the vector of initial damage factors $\mathbf{a}_0^{\mathrm{Si}}$, used as starting point in the optimization process, was selected as the damage factors identified at the previous damage state or zero for state S1. The upper-bound of 95% was selected based on the observed damage in the building, while the lower bound of $\mathbf{a}_0^{\mathrm{Si}}(k)$ was selected considering that the identified effective moduli of elasticity are not expected to increase with increasing damage. The damage factors (relative to the reference FE model or reference state) obtained at different damage states are presented in a bar plot in Figure 5. These results indicate that: (1) the severity of structural damage increases as the building is exposed to stronger earthquake excitations; and (2) the extent of damage decreases rapidly along the height of the building (damage concentrated in the two bottom stories), except for a false alarm in the fourth story at state S4. This large identified damage factor in the fourth story may be due to the facts that (1) the updating parameters (effective moduli of elasticity of substructures) account for the effect of damage in other non-updating elements such as the floor slabs, flange wall, post-tensioned column and the connections between floor slabs and post-tensioned column, and (2) the identified damage factors at state S4 are in general characterized by a higher level of estimation uncertainty than at the previous (lower) damage states. The higher damage estimation uncertainty at state S4 is due to the following facts. (*i*) With increasing level of structural damage, the level of nonlinearity in the structural response increases. Therefore, the assumption that the building behaves as a quasi-linear dynamic system is violated and a linear dynamic model (modal model) is not strictly able to represent well the building, i.e., the modeling error in state S4 is the largest (see Table 5). (*ii*) The optimization algorithm used is not a global optimization algorithm and the probability to converge to a local minimum (which is not the global minimum) increases with increasing difference between the identified modal parameters at

two consecutive damage states such as S3 and S4. To remove local minima as a source of error/ variability, global optimization techniques combining evolution algorithms and gradient methods [25] should be considered in future studies.

Table 5 Comparison of FE computed and experimentally identified modal parameters (ambient vibration test data)

State	Experimentally Identified Natural Frequencies [Hz]			FE Computed Natural Frequencies [Hz]			MAC		
	1^{st}-L mode	2^{nd}-L mode	3^{rd}-L mode	1^{st}-L mode	2^{nd}-L mode	3^{rd}-L mode	1^{st}-L mode	2^{nd}-L mode	3^{rd}-L mode
S0	1.91	10.51	24.51	1.89	10.37	25.03	1.00	0.99	0.96
S1	1.88	10.21	24.31	1.86	10.25	24.91	1.00	0.99	0.97
S2	1.67	10.16	22.60	1.69	9.82	22.43	1.00	0.98	0.98
S3.1	1.44	9.28	21.82	1.46	9.06	21.36	1.00	0.97	0.96
S4	1.02	5.67	15.09	1.01	5.82	15.59	1.00	0.90	0.88

Table 5 presents the natural frequencies computed from the updated FE model at each state considered together with their counterparts identified from ambient vibration data as well as the MAC values between analytical (FE computed) and experimental mode shapes. Note that the analytical mode shapes were truncated to include only the DOFs corresponding to the locations and directions of the accelerometers in order to match the size of the experimental mode shapes. From Table 5, it is observed that: (1) the FE computed natural frequencies and mode shapes of all three vibration modes considered match well their experimentally identified counterparts. (2) The discrepancies between analytical and experimental natural frequencies are in general larger (in both absolute and relative terms) for the second and third modes than for the first mode. This is due to the fact that the identified modal parameters of the second and third modes are not as accurate as (i.e., have a higher estimation uncertainty than) those of the first mode, resulting in smaller

weight factors being assigned to their corresponding residuals (see Table 3). (3) The MAC values between analytical and experimentally identified mode shapes are very close to unity at all damage states except state S4 at which the MAC values for the second and third modes are lower. This will result in a lower level of confidence for the identified damage at state S4.

Case II: Damage Identification Based on White Noise (0.03g RMS) Base Excitation Test Data

In the second case of damage identification, 11 updating parameters (corresponding to 11 substructures) are updated from the reference FE model (at state S0) to states S1, S2, S3.1, and S4. These 11 substructures include the same 10 substructures used in the first case of damage identification, i.e., 6 along the first three stories (two per story) and four along the higher stories (one per story) of the web wall, and one additional substructure consisting of a rotational spring at the base of the web wall to model the flexibility of the shake table system and the rotation at the base of the web wall due to bond slip of the longitudinal reinforcing bars. As already mentioned, the rotation of the base of the web wall played a non-negligible role in the response of the building during the white noise base excitation tests, but was not significant in the ambient vibration tests which were of very low amplitude. At each damage state, the initial damage factors used as starting point in the optimization process are taken as the identified damage factors for the previous damage state or zero for state S1. In updating the reference FE model to states S1 through S4, the dimensionless damage factors were constrained to be in the range $[\mathbf{a}_0^{\mathrm{Si}}(k), 0.95]$ as in Case I. The identified damage factors (relative to the reference state S0) obtained for the web wall and base spring at the various damage states considered are presented in bar plot in Figure 6. These results indicate that: (1) the severity of structural damage increases with the intensity of the earth-

quake excitation; (2) at each damage state, the most severe damage is identified at the first story (top and bottom) and second story (bottom) of the web wall. However, at state S4, severe damage is spuriously identified at the fourth story. The possible explanations for this falsely identified damage factor are the same as in Case I. (3) The rotational spring at the base of the wall is significantly damaged at state S4 due to the development of significant bond-slip in the longitudinal reinforcing bars of the web wall (anchored in the foundation beam) at this damage state.

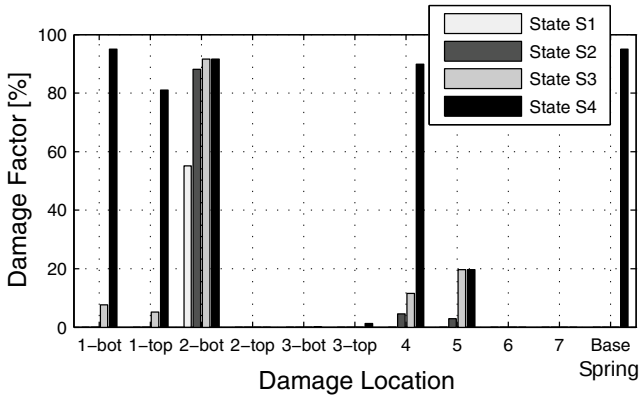

Fig. 6 Identified damage factors at various substructures for damage identification Case II (based on 0.03g RMS white noise test data)

Table 6 presents the natural frequencies computed from the updated FE model at each state considered together with their counterparts identified from the 0.03g RMS white noise base excitation test data as well as the MAC values between FE computed and experimental mode shapes. From Table 6, it is observed that the FE computed natural frequencies and mode shapes of the first and third vibration modes are in good agreement with their experimentally identified counterparts, while the discrepancy between the FE computed and experimentally identified modal parameters of the second mode is significantly larger especially in states S2 and S3.1. This could be due to the proximity of the second mode natural frequency to the oil-column frequency of the shake table resulting to a high estimation uncertainty of the modal parameters of that mode.

Table 6 Comparison of FE computed and experimentally identified modal parameters (0.03g RMS white noise base excitation tests data)

State	Experimentally Identified Natural Frequencies [Hz]			FE Computed Natural Frequencies [Hz]			MAC		
	1^{st}-L mode	2^{nd}-L mode	3^{rd}-L mode	1^{st}-L mode	2^{nd}-L mode	3^{rd}-L mode	1^{st}-L mode	2^{nd}-L mode	3^{rd}-L mode
S0	1.71	11.05	24.31	1.74	10.12	24.20	1.00	0.81	0.95
S1	1.54	10.98	24.28	1.61	9.91	23.85	1.00	0.74	0.96
S2	1.24	11.11	21.59	1.28	9.06	20.46	1.00	0.52	0.73
S3.1	1.14	9.77	19.68	1.18	8.53	19.59	1.00	0.53	0.95
S4	0.88	4.81	13.29	0.85	5.03	13.13	1.00	0.85	0.90

Case III: Damage Identification Based on White Noise (0.05g RMS) Base Excitation Test Data

In the third damage identification case, the same 11 updating parameters used in the previous case are updated at each of states S1, S2, S3.1, and S4. As mentioned earlier, the 0.05g RMS white noise base excitation test was not performed at state S0, therefore the reference FE model calibrated based on the 0.03g RMS white noise test data was used as reference model in this case. In updating the reference FE model to states S1 through S4, the dimensionless damage factors were constrained to be in the range $[\mathbf{a}_0^{Si}(k), 0.95]$ as in the previous cases. The identified damage factors (relative to the reference state) obtained for the web wall and floor slabs at various damage states are presented in bar plot in Figure 7. The results are very similar to those obtained in Case II except for the large damage factor identified at the top of the second story at state S4. This large damage factor may be due to parameter compensation effects, since the effective stiffness of sev-

eral non-updating structural components decreases with increasing amplitude of excitation (i.e., level of response nonlinearity).

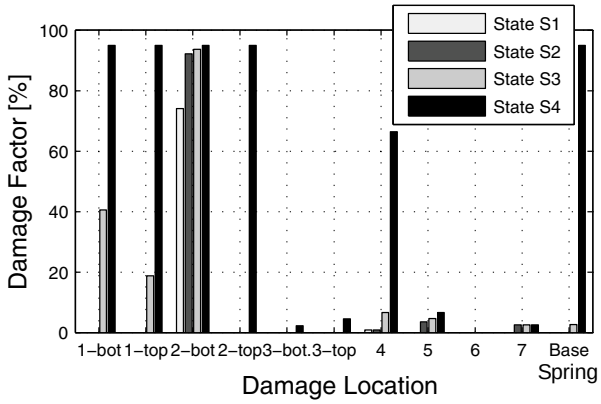

Fig. 7 Identified damage factors at various substructures for damage identification Case III (based on 0.05g RMS white noise test data)

Table 7 Comparison of FE computed and experimentally identified modal parameters (0.05g RMS white noise base excitation test data)

State	Experimentally Identified Natural Frequencies [Hz]			FE Computed Natural Frequencies [Hz]			MAC		
	1^{st}-L mode	2^{nd}-L mode	3^{rd}-L mode	1^{st}-L mode	2^{nd}-L mode	3^{rd}-L mode	1^{st}-L mode	2^{nd}-L mode	3^{rd}-L mode
S1	1.40	11.38	24.29	1.48	9.66	23.69	1.00	0.68	0.95
S2	1.14	10.24	22.46	1.17	8.61	23.50	1.00	0.68	0.94
S3.1	1.06	10.23	18.98	1.10	8.08	19.19	1.00	0.50	0.97
S4	0.81	4.62	13.29	0.79	4.68	14.22	1.00	0.98	0.88

Table 7 presents the FE computed and experimental natural frequencies and the MAC values between FE predicted and experimental mode shapes. From these results, it is observed that similar to the previous damage identification case, the FE predicted and experimental natural frequencies and mode shapes of the first and third vibration modes are in good agreement, while the discrepancy between the FE predicted and experimental modal properties is significantly larger

for the second mode at states S1 to S3.1. Again, this is likely due to the higher estimation uncertainty of this mode.

Fig. 8 Extent of flexure-shear cracking at the first story (plastic-hinge region) of the web wall during EQ4 (at instants of time near maximum base rotation)

Fig. 9 Extent of flexure-shear cracking at the bottom corner of the first story of the web wall during EQ4 (at instant of time near maximum base rotation)

Comparison of Damage Identification Results with Observed Damage

Pictures of the actual damage at the bottom two stories of the web wall at state S4 are shown in Figures 8 through 10. Figures 8 and 9 show a combination of flexure (horizontal) and flexure-shear (inclined) cracks at the first story of the web wall during the seismic test EQ4 (at

instants of time near the maximum base rotation of the web wall). These two figures correspond to two frames taken from two digital movies recorded during seismic test EQ4. During the seismic test EQ4, a lap-splice failure (i.e., debonding between longitudinal steel reinforcement bars and the surrounding concrete) occurred in the web wall at the bottom of the second story on the west side as shown in Figure 10. Figure 11 shows the tensile strain envelopes for the concrete (left) and the longitudinal reinforcement (right) along the first two stories of the web wall over the duration of each of the four seismic tests. The concrete and reinforcement tensile strains were measured using LVDTs and strain gages, respectively. Figures 8 to 10 together with the concrete and longitudinal reinforcement tensile strain envelopes in Figure 11 provide a physical observation/measure of the damage in the wall. The damage identification results obtained in all three cases are consistent with the concentration of actual damage at the bottom two stories of the web wall. However, only in Case I of damage identification, significant loss of stiffness has been identified along the web wall at states S1 and S2. The differences in the identified damage results obtained from the different cases can be due to a number of reasons: (1) different sets of identified modal parameters are used in the three cases, each with a different level of estimation uncertainty; (2) varying degree of modeling error: the assumption of a quasi-linear dynamic system is progressively violated with increasing level of excitation (the ambient vibration data satisfy better the assumption of system linearity and therefore are more appropriate as input for linear FE model updating); (3) different reference/baseline models are used in the three cases of damage identification; (4) different weights are assigned to the various modal residuals in the three cases (due to different modal parameter estimation uncertainties); and (5) different numbers of updating parameters are used in different cases.

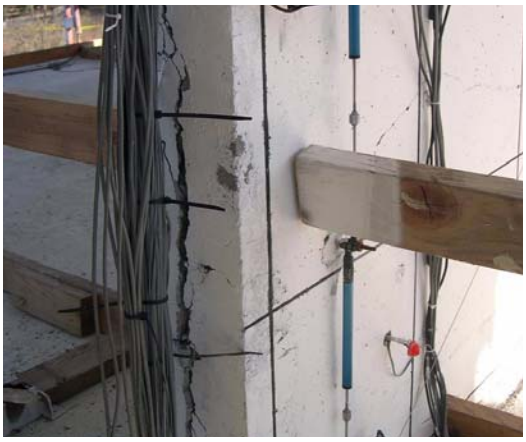

Fig. 10 Splitting crack due to lap-splice failure at the bottom of the second story of the web wall on the west side at state S4 (after EQ4)

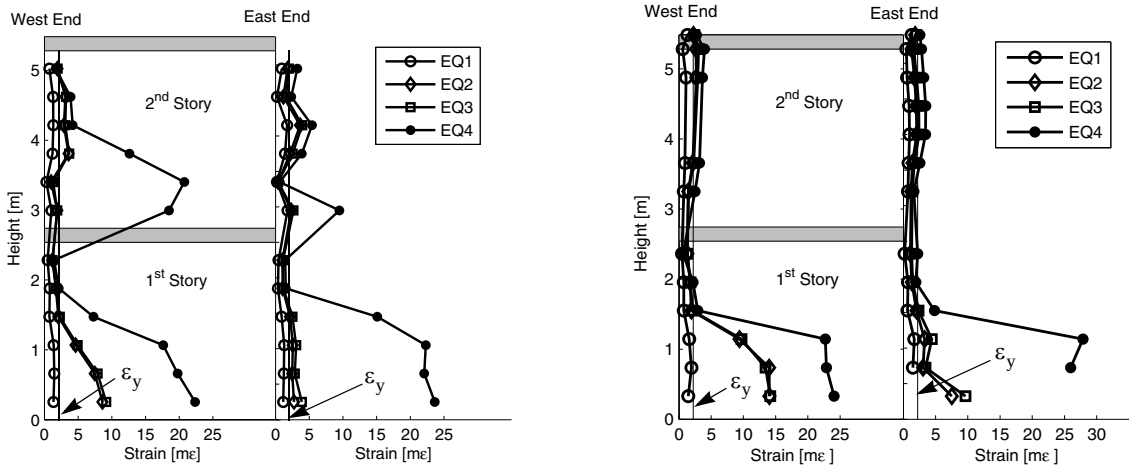

Fig. 11 Tensile strain envelopes of concrete (left) and longitudinal reinforcement (right) along the first two stories of the web wall measured using LVDTs and strain gages in the four seismic tests (ε_y = yield strain of reinforcement steel)

Also by comparing the match between experimentally identified and FE predicted modal parameters after model updating, it is observed that the analytical and experimental modal parameters in Case I are in better agreement than in Cases II and III. This can be explained by the larger modeling error in Cases II and III in which the assumption of quasi-linear dynamic behavior was not as well satisfied as in Case I in spite of the relatively low amplitude of dynamic excitation

(0.03g and 0.05g RMS white noise base acceleration). Therefore, the results from the first case of damage identification are expected to be more accurate.

CONCLUSIONS

In this study, a FE model updating strategy is applied for vibration based damage identification of a full-scale seven-story reinforced concrete building section tested on the UCSD-NEES shake table. Three cases of damage identifications are considered based on different sets of modal parameters identified using (I) ambient vibration test data, (II) 0.03g RMS white noise base excitation test data, and (III) 0.05g RMS white noise base excitation test data. The damage identification results obtained for the three cases do not match exactly, but they are consistent with the actual damage observed in the building which shows a concentration of damage at the bottom two stories of the web wall. The difference in the identified damage results is mainly due to the significant difference in the identified modal parameters used in the three cases. The assumption of a quasi-linear dynamic system is progressively violated with increasing level of excitation. Therefore, the identified modal parameters (especially of the first mode) corresponding to different levels of excitation are significantly different. It is worth noting that the ambient vibration data satisfy better the assumption of system linearity and therefore are more appropriate as input for linear FE model updating. This is confirmed by the fact that the analytical modal parameters obtained from the updated FE models are in better agreement with their experimentally identified counterparts in Case I than in Cases II and III.

With increasing level of structural damage, the level of nonlinearity in the structural response increases (even for the relatively low amplitude 0.03g RMS white noise base excitation). Therefore, with increasing level of damage, the assumption that the building behaves as a quasi-

linear dynamic system is violated and a linear dynamic model (modal model) is not strictly able to represent well the structure. In the future, application of nonlinear FE model updating strategies will resolve these modeling errors caused by structural response nonlinearity. Finally, it should be noted that the success of vibration-based damage identification depends significantly on the accuracy and completeness of the identified modal parameters. Clearly, if estimation uncertainty of the modal parameters is larger than their changes due to damage, it is impossible to resolve/identify the actual damage in the structure. The variability in the damage identification results is mainly driven by the estimation uncertainty of the identified modal parameters and the modeling errors. Therefore, these two sources of uncertainty/variability should be taken into account in order to have higher confidence in the damage identification results. This can be achieved through the use of probabilistic damage identification methodologies such as Bayesian finite element model updating.

ACKNOWLEDGEMENTS

Partial support of this research by Lawrence Livermore National Laboratory with Dr. David McCallen as Program Leader and by the Englekirk Center Board of Advisors are gratefully acknowledged. The authors would like to thank Dr. Marios Panagiotou and Dr. Ozgur Ozcelik as well as the technical staff at the Englekirk Structural Engineering Center for their assistance in collecting the test data used in this study. Any opinions, findings, and conclusions or recommendations expressed in this paper are those of the authors and do not necessarily reflect those of the sponsors.

REFERENCES

[1] Doebling SW, Farrar CR, Prime MB, Shevitz DW. Damage identification in structures and mechanical systems based on changes in their vibration characteristics: a detailed literature survey. Los Alamos National Laboratory Report, LA-13070-MS, Los Alamos NM; 1996.

[2] Doebling SW, Farrar CR, Prime MB. A summary review of vibration-based damage identification methods. The Shock and Vibration Digest 1998; 30(2): 99-105.

[3] Sohn H, Farrar CR, Hemez FM, Shunk DD, Stinemates DW, Nadler BR. A review of structural health monitoring literature: 1996-2001. Los Alamos National Laboratory Report, LA-13976-MS, Los Alamos NM; 2003.

[4] Rytter A. Vibration Based Inspection of Civil Engineering Structures. Ph.D. Dissertation, Department of building Technology and Structural Engineering, Aalborg University, Aalborg, Denmark; 1993.

[5] Salawu OS. Detection of structural damage through changes in frequency: A review. Engineering Structures 1997; 19(9): 718-723.

[6] Pandey AK, Biswas M, Samman MM. Damage detection from changes in curvature mode shapes. Journal of Sound and Vibration 1991; 145(2): 321-332.

[7] Shi ZY, Law SS, Zhang LM. Improved damage quantification from elemental modal strain energy change. Journal of Engineering Mechanics, ASCE 2002; 128(5): 521-529.

[8] Maeck J, De Roeck G. Dynamic bending and torsion stiffness derivation from modal curvatures and torsion rates. Journal of Sound and Vibration 1999; 225(1): 153-170.

[9] Friswell MI, Mottershead JE. Finite element model updating in structural dynamics. Kluwer Academic Publishers, Boston, USA; 1995.

[10] Teughels A, De Roeck G. Structural damage identification of the highway bridge Z24 by finite element model updating. Journal of Sound and Vibration 2004; 278(3): 589–610.

[11] Reynders E, De Roeck G, Bakir PG, Sauvage C. Damage identification on the Tilff bridge by vibration monitoring using optical fibre strain sensors. Journal of Engineering Mechanics, ASCE 2007; 133(2): 185-193.

[12] Panagiotou M, Restrepo JI. A displacement-based method of analysis: Application to the 7-Story full scale building slice tested at UC San Diego. Journal of Structural Engineering, ASCE 2009; under review.

[13] Panagiotou M, Restrepo JI, Conte JP. Shake table test of a 7-Story full scale building slice - Phase I: Rectangular wall. Journal of Structural Engineering, ASCE 2009; under review.

[14] Moaveni B. System and damage identification of civil structures, Ph.D. dissertation, Department of Structural Engineering, University of California, San Diego, CA; 2007.

[15] Ozcelik O, Luco JE, Conte JP, Trombetti TL, Restrepo JI. Experimental characterization, modeling and identification of the NEES-UCSD shake table mechanical system. Earthq. Engng. Struct. Dyn. 2008; 37(2): 243-264.

[16] Teughels A. Inverse modelling of civil engineering structures based on operational modal data, Ph.D. dissertation, Department of Civil Engineering, K.U. Leuven, Belgium; 2003.

[17] Christodoulou K, Papadimitriou C. Structural identification based on optimally weighted modal residuals. Mechanical Systems and Signal Processing 2007; 21(1): 4-23.

[18] Fox RL, Kapoor MP. Rates of change of eigenvalues and eigenvectors. AIAAJ 1968; 6(12): 2426-2429.

[19] Coleman TF, Li Y. An interior, Trust Region approach for nonlinear minimization subject to bounds. SIAM Journal on Optimization 1996; 6(2): 418-445.

[20] MathWorks Inc. Matlab - High performance numeric computation and visualization software, User's Guide. The MathWorks Inc., Natick, MA; 2005

[21] Filippou FC, Constantinides M. FEDEASLab getting started guide and simulation examples. Technical Report NEESgrid-2004-22, http://fedeaslab.berkeley.edu; 2004.

[22] Allman DJ. A quadrilateral finite element including vertex rotations for plane elasticity analysis. International Journal for Numerical Methods in Engineering 1988; 26(3): 717-730.

[23] Batoz JL, Tahar MB. Evaluation of a new quadrilateral thin plate bending element. International Journal for Numerical Methods in Engineering 1982; 18(11): 1655-1677.

[24] He X, Moaveni B, Conte JP, Restrepo JI, Elgamal A. Damage identification of a seven-Story reinforced concrete shear wall building tested on UCSD-NEES shake table. Proc. of 4th World Conference on Structural Control and Monitoring, San Diego, USA; 2006.

[25] Christodoulou K, Ntotsios E, Papadimitriou C, and Panetsos P. Structural model updating and prediction variability using Pareto optimal models. Computer Methods in Applied Mechanics and Engineering 2008; 198(1): 138-149.